

# The mechanism of grape seed oligomeric procyanidins in the treatment of experimental autoimmune encephalomyelitis mice

**Liyuan Xue**

Shanxi Medical University

**Qing Wang**

Shanxi University of Traditional Chinese Medicine

**Zhibin Ding**

Shanxi Medical University

**Qiang Miao**

Shanxi University of Traditional Chinese Medicine

**Yanqing Li**

Shanxi University of Traditional Chinese Medicine

**Lijuan Song**

Shanxi University of Traditional Chinese Medicine

**Yanhua Li**

Shanxi Datong University

**Jiezhong Yu**

Shanxi Datong University

**Yingli Wang**

Shanxi University of Traditional Chinese Medicine

**Cungen Ma** (✉ [macungen@sxtcm.edu.cn](mailto:macungen@sxtcm.edu.cn))

Shanxi University of Traditional Chinese Medicine <https://orcid.org/0000-0003-0049-1658>

---

## Research Article

**Keywords:** grape seed oligomeric procyanidins, network pharmacology, experimental autoimmune encephalomyelitis, multiple sclerosis, MAPK signaling pathway, PI3K-Akt signaling pathway

**Posted Date:** March 31st, 2021

**DOI:** <https://doi.org/10.21203/rs.3.rs-287199/v1>

**License:**   This work is licensed under a Creative Commons Attribution 4.0 International License.

[Read Full License](#)

---



## The mechanism of grape seed oligomeric procyanidins in the treatment of experimental autoimmune encephalomyelitis mice

Liyuan Xue<sup>1#</sup>· Qing Wang<sup>2#</sup>· Zhibin Ding<sup>1</sup>· Qiang Miao<sup>2</sup>· Yanqing Li<sup>2</sup>· Lijuan Song<sup>1,2</sup>· Yanhua Li<sup>3</sup>· Jiezhong Yu<sup>3,4</sup>· Yingli Wang<sup>2</sup>· Cungen Ma<sup>1,2,3</sup>

#The first author.

Liyuan Xue

[19834515620@163.com](mailto:19834515620@163.com)

Qing Wang

[4024771456@163.com](mailto:4024771456@163.com)

Zhibin Ding

[zhibinding2013@163.com](mailto:zhibinding2013@163.com)

Qiang Miao

[miaoq000@163.com](mailto:miaoq000@163.com)

Yanqing Li

[1046107619@qq.com](mailto:1046107619@qq.com)

Lijuan Song

[155360888086@126.com](mailto:155360888086@126.com)

Yanhua Li

[278912829@qq.com](mailto:278912829@qq.com)

Jiezhong Yu

[sxdtyjz@qq.com](mailto:sxdtyjz@qq.com)

✉ Yingli Wang.

[wyl@sxtcm.edu.cn](mailto:wyl@sxtcm.edu.cn)

✉ Cungen Ma

[macungen@sxtcm.edu.cn](mailto:macungen@sxtcm.edu.cn)

<sup>1</sup> Department of Neurology, The First Clinical Medical College, Shanxi Medical University, Taiyuan, 030001, China.

<sup>2</sup> Research Center of Neurobiology, The Key Research Laboratory of Benefiting Qi for Acting Blood Circulation Method to Treat Multiple Sclerosis of State Administration of Traditional Chinese Medicine, Shanxi University of Chinese Medicine, Jinzhong, 030619, China.

<sup>3</sup> Institute of Brain Science, Shanxi Key Laboratory of Inflammatory Neurodegenerative Diseases, Shanxi Datong University, Datong, 037009, China.

<sup>4</sup> Department of Neurology, Datong Fifth People's Hospital, Datong, 037009, China.

## **Abstract**

**Objective** This study aims to investigate the mechanism of grape seed oligomeric procyanidins (GPC) in the treatment of experimental autoimmune encephalomyelitis (EAE) mice, providing pharmacodynamic materials for drug development in the treatment of multiple sclerosis (MS).

**Methods** The constituents which have nerve protective effect in GPC were collected through literature retrieval. We used PharmMapper and STITCH database to predict drug targets, GeneCards and OMIM database to predict MS-related genes. Targets of GPC treating MS were obtained from intersected targets between drug and disease. The GO functional enrichment and KEGG pathway enrichment analysis were performed by DAVID database. EAE mouse model was used to study the therapeutic mechanism of GPC. **Results** Forty-two targets were discovered to be related to the process of GPC treating MS. KEGG enriched a total of 32 pathways. The pharmacological experiment showed that GPC improved the clinical symptoms of EAE mice, inhibited the expression of indicators of oxidative stress and inflammatory response in CNS, and decreased the expression of P-Akt, P-ERK, and P-JNK. **Conclusion** The therapeutic effect of GPC in EAE mice is associated with the suppression of MAPK and PI3K-Akt signaling pathways, providing a theoretical basis for the application of GPC in MS.

**Keywords:** grape seed oligomeric procyanidins, network pharmacology, experimental autoimmune encephalomyelitis, multiple sclerosis, MAPK signaling pathway, PI3K-Akt signaling pathway.

## **1. Materials and methods**

### **2. Introduction**

Multiple sclerosis (MS) is an inflammatory demyelinating disease of the central nervous system (CNS), affecting over 2 million people worldwide, the main pathological features of which include inflammation, demyelination, axonal loss, and glial cell proliferation (Reich et al. 2018). Experimental autoimmune encephalomyelitis (EAE) is the classical animal model for MS's relevant research and exhibits similar characteristics of MS (Robinson et al. 2014). At present, the drugs to treat MS are mainly hormones and immunosuppressants, with many side effects and are of high prices (Filippini et al. 2017). Therefore, many scholars are committed to find active ingredients from natural compounds and explore new therapeutic drugs (Sanadgol et al. 2017).

Procyanidins (PC), a class of representational flavanols extracted from the skins, shells, and seeds of plants, are characterized by low toxicity, high efficiency, and bioavailability (Rodriguez-Perez et al. 2019). PC is polymerized from catechins or epicatechins with different degrees of polymerization and classified as procyanidolic oligomers (OPC) (dimer to tetraomers) and procyanidolic polymers (PPC) (polymers above pentapolymeric) (Gao and Dong 2009). The grape seeds contain the most abundant PC and show excellent effects of anti-oxidation, anti-inflammation, anti-cancer, and neuroprotection, etc. (Bai et al. 2019). Based on the above characteristics, some studies have determined its effect on several CNS diseases, including Alzheimer's disease and cerebrovascular disease and showed good therapeutic effects (Kong et al. 2017; Matsuda et al. 2014; Wu et al. 2015; Zhao et al. 2019). However, there are few experiments on the treatment of MS. Also, network pharmacology can systematically elucidate the mechanism of drug's actions from multiple levels, such as targets and pathways (Liu and Sun 2012). So this study was designed to analyze the mechanism of GPC in the treatment of EAE mice by the combination of network pharmacology and experimental verification to provide basis for the clinical application of GPC in the treatment of MS. The specific process is shown in Fig. 1.

#### **2.1 The screening of active ingredients and the prediction of targets for GPC**

We used the PubMed database (<https://pubmed.ncbi.nlm.nih.gov/>) to retrieve the references and collect active compounds that protect the nerves in GPC. Then, target proteins were obtained from

databases of PharmMapper (<http://www.lilab-ecust.cn/pharmmapper/>) and STITCH (<http://stitch.embl.de/>). The targets from the PharmMapper database were filtered by a score > 0.9. Targets are standardized in the UniProt database (<http://www.uniprot.org/>). Cytoscape 3.6.1 software was used to map the 'drug-target' network.

## 2.2 Acquisition of MS-related target genes

GeneCards database (<https://www.genecards.org/>) and OMIM database (<https://omim.org/>) were employed to detect MS-related target genes by searching 'multiple sclerosis'. The targets from the GeneCards database were filtered by a relevance score > 6.705.

## 2.3 Construction of network and topological analysis

We used the Excel function to take the intersection between drug and disease targets to obtain therapeutic targets of GPC against MS, and drew Venn diagrams in the bioinformatics platform (<https://www.bioinformatics.com.cn>). We introduced these common genes into STRING 11.0 database (<https://string-db.org/>) to collect the functional relationship between the targets. Resultant data were introduced into Cytoscape 3.6.1 software to establish the PPI network among the common targets. Cytoscape 3.6.1 software was used to map the 'drug-target-disease' network. Network analyzer in Cytoscape was utilized in analyzing topological parameters of mean and maximum degrees of freedom in PPI network among the common targets.

## 2.4 Biological function and pathway enrichment analyses of the core targets

The core targets obtained in 2.3 were imported into DAVID 6.8 (<http://david.nifcrf.gov/>) database in the format of GeneSymbol for GO analysis and KEGG pathway enrichment analysis. The important biological functions and core pathways were screened out ( $P < 0.05$ , count  $\geq 7$ ) to draw the bubble diagram.

## 2.5 Experimental animals and the establishment of the EAE model

A total of 18 female C57BL/6 mice, 10-12 weeks old, were purchased from Vital River Laboratory Animal Technology Co. Ltd. (Beijing, China), and were raised in the condition of 25°C without

pathogenic bacteria. All animal experiments were approved by the Council for Laboratory and Ethics Committee of the Shanxi University of Chinese Medicine, Taiyuan, China.

Myelin oligodendrocyte glycoprotein peptide-35-55 (MOG35–55, MEVGWYRSPFSRVVHL-YRNGK, CL. Bio-Scientific Company, Shanghai, China) (200µg/ mouse) dissolved in normal saline (NS) was fully emulsified with Mycobacterium tuberculosis H37R (BD Difco, Detroit, MI, USA) (400µg/mouse) completely dissolved in complete Freund's adjuvant (Sigma, USA). Each mouse was injected with antigen emulsion to induce EAE in the dorsal lumbosacral bulking region. The day of immunization was recorded as day 0 post-immunization (p.i.). Each mouse was intraperitoneally injected with 300ng pertussis toxin (PTX, List Labs, USA) on day 0 and day 2 p.i. Animals were evaluated for clinical scores every other day in a double-blinded fashion by at least two investigators.

## **2.6 Administration of GPC and the evaluation of clinical score**

Eighteen mice were divided into the EAE control group (n=12) and the GPC treatment group (n=6). GPC was purchased from Tianjin Jianfeng Natural Product R&D Co. Ltd. (Tianjin, China). From day 3 p.i. to day 28 p.i., the GPC treatment mice group were intragastrically administered with GPC (Gong et al. 2020; Yoo et al. 2011) (50 mg·kg<sup>-1</sup>·day<sup>-1</sup>). The control mice received vehicle only in a similar manner.

The international standard 5-point method was adopted to observe and evaluate the symptoms of the experimental mice at regular intervals from day 0 p.i.. The evaluation criteria were as follows: 0 point were scored for the absence of any clinical symptoms; 1 point for tottering gait or loss of tension with tail; 2 points for gait with partial paralysis of hindlimbs and the tail (ataxia); 3 points for total paralysis of unilateral hind limb and tail scored; 4 points for total paralysis of both hind limbs and tail scored; 5 points for near death or death. Symptoms ranged between the two criteria were measured as ± 0.5 points.

## **2.7 The collection of samples and analysis using different methods**

On the 28 p.i., 10% chloral hydrate (0.2 ml/piece) was injected intraperitoneally for anesthesia in the sterile condition. Then, half of the mice of two groups were perfused intracardially with NS followed by 4% paraformaldehyde (PFA) in PBS (0.01 M, pH = 7.4). The spinal cord of mice was

quickly extracted and dehydrated by soaking in sucrose solution of 15%, 25%, and 30% for 24 hours, respectively. The coronal sections of the spinal cord (10  $\mu$ m) were obtained using a cryostat microtome (Leica CM1850, Germany) and stored at 4 °C for Haematoxylin/eosin (H&E), Luxol fast blue (LFB) and Immunofluorescence staining. The rest of the mice were perfused intracardially with NS only. The spinal cords were removed for ELISA and western blot.

### **2.7.1 Histological staining**

Pathological changes in the spinal cords were detected by H&E and LFB staining. For H&E staining, the slides were immersed in haematoxylin solution for 2 min, in water for 1 min, and then in eosin solution for 10 min. Then, differentiation was performed in 1% hydrochloric acid ethanol for 10 s. For LFB staining, the slides were immersed in LFB at 56 °C for 16 h. The excessive blue stain was removed in 95% ethanol and distilled water, and the slides were differentiated in lithium carbonate solution for 15 s. After being washed with distilled water and 80% alcohol, the slides were dehydrated with gradient ethanol and finally mounted with neutral balsam. A set of matched serial sections (3 sections/animal) were imaged under a light microscope (DM4000B, Leica, Germany). The number of infiltrating cells (>20 mononuclear cells/field) was observed by H&E staining, and the integrated optical density of LFB staining in the spinal cord was measured in the lesion area/field using ImagePro Plus 6.0.

### **2.7.2 Immunofluorescence staining**

Sections of the spinal cord were sealed with 1% BSA at room temperature for 30 min. Sections of the two groups were added with 1%BSA primary anti-MBP (1:500), respectively, and incubated overnight at 4°C. The next day, PBST was rinsed and sectioned for 3 times, then the corresponding secondary antibody was added and incubated at room temperature for 1 hour. Rinse and slice PBST for 3 times and incubate DAPI for 5 min. Glycerin was used to seal the slides, and the slides were observed by blind fluorescence microscopy. The optical density was measured by Image-Pro Plus 6.0.

### **2.7.3 ELISA**

The levels of oxidative stress and inflammatory response indicators, including superoxide dismutase

(SOD), malondialdehyde (MDA), reactive nitrogen species (RNS), reactive oxygen species (ROS), INF- $\gamma$ , IL-17, IL-1 $\beta$ , IL-6, and TNF- $\alpha$ , in the supernatant of the spinal cord were measured by ELISA kit according to the manufacture's instructions. The OD value (450 nm) was read by Multiskan Spectrum, and the results were expressed as pg/ml.

#### **2.7.4 Western blot**

Spinal cords were homogenized with a micro content motor-operated tissue homogenizer (Kimble Kontes, USA), using protein extraction kit (Sigma, USA) supplemented with a cocktail of protease inhibitors. The homogenates were centrifuged at 13,000g for 20 min at 4 °C, and the supernatants were collected. The protein concentration was determined by BCA method. Equal amounts of protein (30  $\mu$ g) were separated by SDS-PAGE and electroblotted onto PVDF membrane (Immobilon-P, Millipore, USA). After non-specific binding was blocked with 5% non-fat dry milk, membranes were incubated at 4 °C overnight with anti-MBP, anti-Akt, anti-ERK, anti-JNK, anti-P-Akt, anti-P-ERK, anti-P-JNK and anti- $\beta$ -actin (1:1000, Bioworld, USA). After washing the membrane the next day, it should be incubated with the second antibody at room temperature for 2 hours. Bands were visualized with an enhanced chemiluminescence (ECL) system (GE Healthcare Life Sciences, USA).

#### **2.8 Statistical method**

The GraphPadPrism 7.0 statistical analysis software (Cabinet Information Technology Co., Ltd. Shanghai, China) was used for data analysis. All the data were first checked to see if it is normally distributed. One-way analysis of variance (ANOVA) was performed and followed by Tukey's posttest for multiple comparisons or Student's t-test for comparisons of 2 groups. Results are presented as the mean  $\pm$  SEM. P<0.05 was considered to be statistically significant.

### **3. Results**

#### **3.1 Main active compound and targets of GPC**

Seven active ingredients (Bernatova 2018; Fu et al. 2019; Lee and Yune 2014; Mizuno et al. 2019;

Song et al. 2019; Sutcliffe et al. 2017; Syed Hussein et al. 2015) were selected through literature reviews, as shown in Tab. 1. Seventy-eight drug targets were predicted in PharmMapper and STITCH databases, and potential targets were standardized in the Uniprot database. Cytoscape 3.6.1 software was used to build the 'compound-target' network, and the results were shown in Fig. 2. The network consisted of 85 nodes and 215 edges.

### 3.2 The prediction of disease target genes and the building of networks

We collected 1701 MS-related targets by retrieving 'Multiple sclerosis' in GeneCards database and OMIM database, respectively (duplicates were removed). The drug's target proteins and the disease's target genes were intersected to obtain the common targets, and the Venn diagram was drawn using the Micro-generative communication platform, as shown in Fig. 3A. The PPI network was constructed by using STRING database and Cytoscape 3.6.1, as shown in Fig. 3B. The network (hide 1 disconnected node in the network) consists of 41 nodes and 260 edges. The degree value represents the order of importance in the network: the larger value, the more important target. The mean degree value is 12.4, and AKT1's degree value is maximum (32). The nodes represent common targets, while the edges represent the interaction relationship between targets. It can be seen from the network that AKT1, CASP3, MAPK1, EGFR, PTGS2, MAPK3, MAPK14, and MAPK8 were the core targets of GPC in the treatment of MS. Cytoscape 3.6.1 software was used to construct the 'compound-target-disease' network, as shown in Fig. 3C. The network consisted of 50 nodes and 165 edges.

### 3.3 Enrichment analysis

GO belongs to the classification system of gene function, which has three branches, including biological process (BP), cellular component (CC) and molecular function (MF). After enrichment analysis of targets, GO biological function showed that the pharmacodynamic mechanism of GPC in treating EAE mice involved 27 items ( $P < 0.05$ ,  $\text{count} \geq 7$ ), which include 10 biological processes (peptidyl-serine phosphorylation, response to lipopolysaccharide, positive regulation of cell proliferation, positive regulation of gene expression, positive regulation of transcription, signal transduction, protein phosphorylation, positive regulation of transcription from RNA polymerase II

promoter, apoptotic process, transcription, and DNA-templated), 10 cell compounds (extracellular space, cytosol, nucleoplasm, mitochondrion, cytoplasm, extracellular region, nucleus, extracellular exosome, plasma membrane and intracellular) and 7 molecular functions (enzyme binding, protein binding, kinase activity, protein serine/threonine kinase activity, ATP binding, protein kinase activity, and zinc ion binding). The results are shown in the Fig. 4A. In this study, 32 signaling pathways ( $P<0.05$ , count $\geq 7$ ) were screened out, related to tumor (such as TNF signaling pathway), inflammation (such as MAPK signaling pathway), viral infection (such as Hepatitis B), etc. The results are shown in Fig. 4B.

### **3.4 GPC alleviated clinical symptoms and central inflammation and protected myelin sheath in EAE mice**

On day 11 p.i., the mice developed the disease. On day 28 p.i., samples were collected. The pattern diagram is shown in Fig 5A. Compared with the EAE control group, the clinical scores of mice in the GPC treatment group were lower (Fig. 5B). By histopathological analysis (Fig. 5C), H&E staining revealed reduced infiltration of inflammatory cells in mice of the GPC treatment group compared with that of the EAE control group ( $P<0.05$ ). LFB staining showed that compared with EAE control mice, the demyelination of the GPC treatment group was reduced ( $P<0.01$ ). Immunofluorescence staining (Fig. 5D) showed that MBP mean fluorescence IOD of the GPC treatment group was higher than the EAE control group ( $P<0.05$ ). Western blotting (Fig. 5E) showed that MBP relative grey value of the GPC treatment group was lower than the EAE control group ( $P<0.05$ ).

### **3.5 Effects of GPC on markers of oxidative stress and inflammatory response**

GPC has good antioxidant stress and anti-inflammatory effects. Therefore, ELISA detected the expression of related indexes in spinal cord tissue of mice. As shown in Fig. 6A, there was no significant difference in SOD expression between the two groups. Compared with the control group, the expression of MDA ( $P<0.01$ ), RNS ( $P<0.01$ ) and ROS ( $P<0.001$ ) in the GPC treatment group were decreased. As shown in Fig. 6B, the expressions of INF- $\gamma$  ( $P<0.05$ ), IL-17 ( $P<0.01$ ), IL-1 $\beta$

( $P < 0.01$ ), IL-6 ( $P < 0.001$ ), and TNF- $\alpha$  ( $P < 0.01$ ) in the GPC treatment group were inhibited.

### 3.6 Inhibition of inflammatory signaling pathways by GPC

In order to verify the anti-inflammatory mechanism of GPC in EAE mice, we analyzed the regulatory effect of GPC on MAPK and PI3K-Akt signaling pathways according to the results of KEGG enrichment analysis. Western blot was performed to detect Akt, JNK, and ERK and their phosphorylation levels, and it is found that GPC could inhibit the phosphorylation of Akt, JNK, and ERK (Fig. 7).

## 4. Discussion

At present, the pathogenesis of MS is still unclear, and inflammatory response is a critical process in its pathogenesis (Lassmann 2018). The current treatments for MS mainly include anti-inflammatory and immunomodulation, and some Western medicines have side effects (Gholamzad et al. 2019). Traditional Chinese medicine has multiple targets and overall regulation (Li et al. 2016), but is complicated and challenging to study due to its multi-compounds and multi-targets synergistic effect. Network pharmacology shows biologically active compounds, predicts drug targets, distinguishes the priority of disease-related genes, further establishes 'drug-target-disease' network, and provides a theoretical basis for the modernization of traditional Chinese medicine and the development of new drugs with its holistic way of thinking and strong predictive ability (Yuan et al. 2017). This study aims to analyze the potential mechanism of GPC in the treatment of MS by network pharmacology and animal experiments.

At first, we identified 7 active compounds of GPC acting on 42 targets to treat MS, indicating that the treatment of MS by GPC is the result of the synergistic effect of multiple compounds and multiple targets. AKT1, MAPK1, MAPK3, and other targets with high degree values were found from the PPI network, showing that these targets may be the core targets in the process of GPC treating MS. GO enrichment analysis demonstrated that GPC's therapy for MS was achieved by regulating cell proliferation, regulation of transcription, signal transduction, protein phosphorylation, and apoptotic process. The KEGG pathway enriched 32 pathways related to several biological processes, such as oxidative stress, inflammation, tumor, virus infection, and other functions. In the enrichment results of the KEGG pathway, after screening by the  $P$ -value and the count value, we

observed that the MAPK and the PI3K-Akt signaling pathways are two very important target pathways. These two pathways are related to cell proliferation, stress, inflammation, and apoptosis (da Silva et al. 2020; Lake et al. 2016), therefore, closely related to the occurrence and development of MS. In some previous studies, researchers have found that the abnormal activation of these two pathways is strongly related to the degree of inflammatory cell infiltration and demyelination in the EAE model (Liu et al. 2017; Suo et al. 2019). Besides, GPC, an excellent anti-inflammatory substance and antioxidant, can inhibit these two pathways, suggesting that it may have a potential therapeutic effect on MS.

Based on the above findings, we investigated the therapeutic effect of GPC on EAE and its influence on the above two signaling pathways. As expected, we found that GPC improved the clinical symptoms, reduced central inflammatory cell infiltration and demyelination, and inhibition of expression of relevant oxidative stress markers and inflammatory factors, which are related to the MAPK and PI3K-Akt signaling pathways by down-regulating phosphorylation of AKT, JNK and ERK. MAPK signaling pathway includes p38MAPK, JNK and ERK. It is reported that all MAPK kinases were activated in the EAE-affected spinal cord, and P-ERK and P-JNK were more evident (Shin et al. 2003). Among them, Akt is an important downstream molecule of the PI3K-Akt signaling pathway (Norrmén and Suter 2013). In the rats with D-galactose-induced Alzheimer's disease, the density of hippocampus synapses and the P-Akt level decreased. However, after the external interventions, the clinical symptoms of the above animal models improved, and the levels of corresponding protein phosphorylation in the lesions were down-regulated (Lu et al. 2017; Zheng et al. 2020), which are consistent with our experimental results.

In addition, the blood-brain barrier (BBB) between blood and brain tissue, which is composed of brain capillary endothelial cells, basal membrane, and the footplate of astrocyte protuberance (Liebner et al. 2018), may maintain the homeostasis of the CNS and protect the nerve tissue from toxins and pathogens (Daneman and Prat 2015). Whether drugs can pass through the BBB is the key to the treatment of central nervous system diseases. However, there were few studies on the pharmacokinetics of GPC, with mixed reviews on its ability to penetrate the BBB. According to the TCMSP and SwissTargetPrediction databases, most of the PC are difficult to penetrate the BBB, but can effectively relieve symptoms of CNS diseases (Kong et al. 2017; Yang et al. 2020; Zhao et al. 2019), which is considered to be related to the damage of the BBB caused by the disease. And it has

been confirmed that there is BBB destruction in EAE mice and MS patients (Fabis et al. 2007). Therefore, in the present study, we investigated the therapeutic effect of GPC on EAE, and the results proved that GPC has therapeutic effects. However, because the specific pathogenesis of EAE and MS are different, and EAE is a central inflammatory injury caused by artificially inducing peripheral immunity, and whether targets of GPC is in the center or the periphery needs to be further studied.

## **5. Summary**

In this study, the active components, targets and action pathways of GPC were analyzed and validated by network pharmacology and experimental verification methods. The results showed that GPC against MS exerts its efficacy through the synergistic effect of multiple components, multiple targets and multiple pathways. The later experimental verification confirmed that GPC's therapeutic effect plays an anti-inflammatory role by inhibiting the expression of inflammatory factors through MAPK signaling pathway and PI3K-Akt signaling pathway.

## **Acknowledgments**

This work was supported by grants from the National Natural Science Foundation of China (81473577,81903596), Science and technology innovation project of Shanxi Colleges (2019L0728), Cultivation Project of Shanxi University of Chinese Medicine (2019PY130, 2020PY-JC-14), Open Project of the Key Laboratory of Medicinal Resources and Natural Pharmaceutical Chemistry, The Ministry of Education (2019004), College of Life Sciences, Shaanxi Normal University.

## **Conflict of interest**

None of the authors has any potential financial and non-financial conflict of interest related to this manuscript.

## **Reference**

1. Bai R, Cui Y, Luo L, Yuan D, Wei Z, Yu W et al. A semisynthetic approach for the simultaneous reaction of grape seed polymeric procyanidins with catechin and epicatechin to obtain oligomeric procyanidins in large scale. *Food Chem.* 2019, 278:609-616.

<https://doi.org/10.1016/j.foodchem.2018.11.091>

2. Bernatova I. Biological activities of (-)-epicatechin and (-)-epicatechin-containing foods: Focus on cardiovascular and neuropsychological health. *Biotechnol Adv.* 2018, 36(3):666-681. <https://doi.org/10.1016/j.biotechadv.2018.01.009>
3. da Silva LC, Lima IVA, da Silva MCM, Corrêa TA, de Souza VP, de Almeida MV et al. A new lipophilic amino alcohol, chemically similar to compound FTY720, attenuates the pathogenesis of experimental autoimmune encephalomyelitis by PI3K/Akt pathway. *Int Immunopharmacol.* 2020, 88:106919. <https://doi.org/10.1016/j.intimp.2020.106919>
4. Daneman R, Prat A . The blood-brain barrier. *Cold Spring Harb Perspect Biol.* 2015, 7(1):a020412. <https://doi.org/10.1101/cshperspect.a020412>
5. Fabis MJ, Scott GS, Kean RB, Koprowski H, Hooper DC. Loss of blood-brain barrier integrity in the spinal cord is common to experimental allergic encephalomyelitis in knockout mouse models. *Proc Natl Acad Sci U S A.* 2007, 104:5656-5661. <https://doi.org/doi:10.1073/pnas.0701252104>
6. Filippini G, Del Giovane C, Clerico M, Beiki O, Mattoscio M, Piazza F et al. Treatment with disease-modifying drugs for people with a first clinical attack suggestive of multiple sclerosis. *Cochrane Database Syst Rev.* 2017, 4:CD012200 <https://doi.org/10.1002/14651858.CD012200.pub2>
7. Fu B, Zeng Q, Zhang Z, Qian M, Chen J, Dong W et al. Epicatechin Gallate Protects HBMVECs from Ischemia/Reperfusion Injury through Ameliorating Apoptosis and Autophagy and Promoting Neovascularization. *Oxid Med Cell Longev.* 2019, 2019:7824684. <https://doi.org/10.1155/2019/7824684>
8. Gao Y, Dong Z. Progress on study of pharmacological effects of procyanidins. *Zhongguo Zhong Yao Za Zhi.* 2009, 34(6):651-655
9. Gholamzad M, Ebtekar M, Ardestani MS, Azimi M, Mahmodi Z, Mousavi MJ et al. A comprehensive review on the treatment approaches of multiple sclerosis: currently and in the future. *Inflamm Res.* 2019, 68(1):25-38. <https://doi.org/10.1007/s00011-018-1185-0>
10. Gong X, Xu L, Fang X, Zhao X, Du Y, Wu H et al. Protective effects of grape seed procyanidin on isoflurane-induced cognitive impairment in mice. *Pharm Biol.* 2020, 58(1):200-. 207. <https://doi.org/10.1080/13880209.2020.1730913>
11. Kong X, Guan J, Gong S, Wang R. Neuroprotective Effects of Grape Seed Procyanidin Extract on

- Ischemia-Reperfusion Brain Injury. Chin Med Sci J. 2017, 32(2):92-99.  
<https://doi.org/10.24920/J1001-9294.2017.020>
12. Lake D, Corrêa SA, Müller J. Negative feedback regulation of the ERK1/2 MAPK pathway. Cell Mol Life Sci. 2016, 73(23):4397-4413. <https://doi.org/10.1007/s00018-016-2297-8>
  13. Lassmann H. Multiple Sclerosis Pathology. Cold Spring Harb Perspect Med. 2018, 8(3).  
<https://doi.org/10.1101/cshperspect.a028936>
  14. Lee JY, Yune TY. Ghrelin inhibits oligodendrocyte cell death by attenuating microglial activation. Endocrinol Metab (Seoul) . 2014, 29(3):371-378. <https://doi.org/10.3803/EnM.2014.29.3.371>
  15. Li L, Zhang L, Yang CC. Multi-Target Strategy and Experimental Studies of Traditional Chinese Medicine for Alzheimer's Disease Therapy. Curr Top Med Chem. 2016, 16(5):537-548.  
<https://doi.org/10.2174/1568026615666150813144003>
  16. Liebner S, Dijkhuizen RM, Reiss Y, Plate KH, Agalliu D, Constantin G. Functional morphology of the blood-brain barrier in health and disease. Acta Neuropathol.2018, 135(3):311-336.  
<https://doi.org/10.1007/s00401-018-1815-1>
  17. Liu SQ, Zhang ML, Zhang HJ, Liu FZ, Chu RJ, Zhang GX, et al. Matrine promotes oligodendrocyte development in CNS autoimmunity through the PI3K/Akt signaling pathway. Life Sci. 2017, 180:36-41. <https://doi.org/10.1016/j.lfs.2017.05.010>
  18. Liu ZH, Sun XB. Network pharmacology: new opportunity for the modernization of traditional Chinese medicine. Yao Xue Xue Bao. 2012, 47(6):696-703
  19. Lu L, Zhang X, Tong H, Zhang W, Xu P, Qu S. Central Administration of 5Z-7-Oxozeanol Protects Experimental Autoimmune Encephalomyelitis Mice by Inhibiting Microglia Activation. Front Pharmacol. 2017, 8:789. <https://doi.org/10.3389/fphar.2017.00789>
  20. Matsuda N, Ohkuma H, Naraoka M, Munakata A, Shimamura N, Asano K. Role of oxidized LDL and lectin-like oxidized LDL receptor-1 in cerebral vasospasm after subarachnoid hemorrhage. J Neurosurg. 2014, 121(3):621-630. <https://doi.org/10.3171/2014.5.JNS132140>
  21. Mizuno M, Mori K, Misawa T, Takaki T, Demizu Y, Shibanuma M, et al. Inhibition of  $\beta$ -amyloid-induced neurotoxicity by planar analogues of procyanidin B3. Bioorg Med Chem Lett. 2019, 29(8):2659-2663. <https://doi.org/10.1016/j.bmcl.2019.07.038>
  22. Norrmén C, Suter U. Akt/mTOR signalling in myelination. Biochem Soc Trans. 2013, 41(4):944-950. <https://doi.org/10.1042/bst20130046>

23. Reich DS, Lucchinetti CF, Calabresi PA. Multiple Sclerosis *N Engl J Med*. 2018, 378(2):169-180.  
<https://doi.org/10.1056/NEJMra1401483>
24. Robinson AP, Harp CT, Noronha A, Miller SD. The experimental autoimmune encephalomyelitis (EAE) model of MS: utility for understanding disease pathophysiology and treatment. *Handb Clin Neurol*. 2014, 122:173-189. <https://doi.org/10.1016/b978-0-444-52001-2.00008-x>
25. Rodriguez-Perez C, Garcia-Villanova B, Guerra-Hernandez E, Verardo. Grape Seeds Proanthocyanidins: An Overview of In Vivo Bioactivity in Animal Models. *Nutrients*. 2019, 11(10). <https://doi.org/10.3390/nu11102435>
26. Sanadgol N, Zahedani SS, Sharifzadeh M, Khalseh R, Barbari GR, Abdollahi M. Recent Updates in Imperative Natural Compounds for Healthy Brain and Nerve Function: A Systematic Review of Implications for Multiple Sclerosis. *Curr Drug Targets*. 2017, 18(13):1499-1517.  
<https://doi.org/10.2174/1389450118666161108124414>
27. Shin T, Ahn M, Jung K, Heo S, Kim D, Jee Y et al. Activation of mitogen-activated protein kinases in experimental autoimmune encephalomyelitis. *J Neuroimmunol*. 2003, 140(1-2):118-125. [https://doi.org/10.1016/s0165-5728\(03\)00174-7](https://doi.org/10.1016/s0165-5728(03)00174-7)
28. Song JH, Lee HJ, Kang KS. Procyanidin C1 Activates the Nrf2/HO-1 Signaling Pathway to Prevent Glutamate-Induced Apoptotic HT22 Cell Death. *Int J Mol Sci*. 2019, 20(1).  
<https://doi.org/10.3390/ijms20010142>
29. Suo N, Guo YE, He B, Gu H, Xie X. Inhibition of MAPK/ERK pathway promotes oligodendrocytes generation and recovery of demyelinating diseases. *Glia*. 2019, 67(7):1320-1332.  
<https://doi.org/10.1002/glia.23606>
30. Sutcliffe TC, Winter AN, Punessen NC, Linseman DA. Procyanidin B2 Protects Neurons from Oxidative, Nitrosative, and Excitotoxic Stress. *Antioxidants (Basel)*. 2017, 6(4).  
<https://doi.org/10.3390/antiox6040077>
31. Syed Hussein SS, Kamarudin MN, Kadir HA. (+)-Catechin Attenuates NF- $\kappa$ B Activation Through Regulation of Akt, MAPK, and AMPK Signaling Pathways in LPS-Induced BV-2 Microglial Cells. *Am J Chin Med*. 2015, 43(5):927-952. <https://doi.org/10.1142/s0192415x15500548>
32. Wu S, Yue Y, Li J, Li Z, Li X, Niu Y et al. Procyanidin B2 attenuates neurological deficits and blood-brain barrier disruption in a rat model of cerebral ischemia. *Mol Nutr Food Res*. 2015, 59(10):1930-1941. <https://doi.org/10.1002/mnfr.201500181>

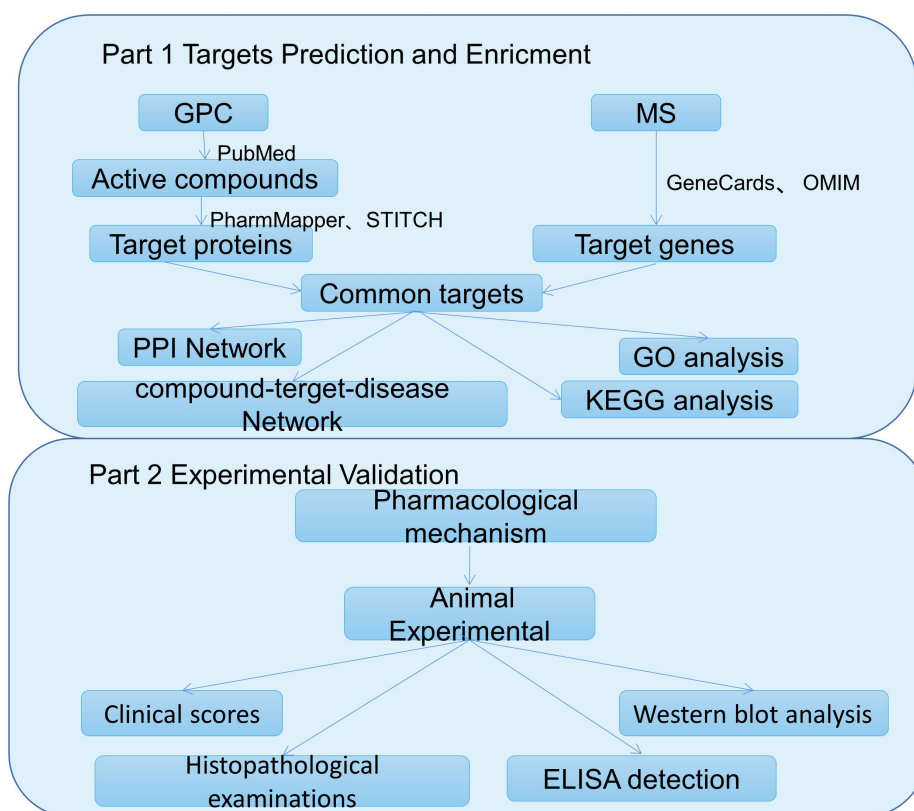
33. Yang B, Sun Y, Lv C, Zhang W, Chen Y. Procyanidins exhibits neuroprotective activities against cerebral ischemia reperfusion injury by inhibiting TLR4-NLRP3 inflammasome signal pathway. *Psychopharmacology (Berl)*. 2020, 237:3283-3293. <https://doi.org/10.1007/s00213-020-05610-z>
34. Yoo DY, Kim W, Yoo KY, Lee CH, Choi JH, Yoon YS et al. Grape seed extract enhances neurogenesis in the hippocampal dentate gyrus in C57BL/6 mice. *Phytother Res*. 2011, 25(5):668-674. <https://doi.org/10.1002/ptr.3319>
35. Yuan H, Ma Q, Cui H, Liu G, Zhao X, Li W, et al. How Can Synergism of Traditional Medicines Benefit from Network Pharmacology? *Molecule*. 2017, 22(7). <https://doi.org/10.3390/molecules22071135>
36. Zhao S, Zhang L, Yang C, Li Z, Rong S. Procyanidins and Alzheimer's Disease. *Mol Neurobiol*. 2019, 56(8):5556-5567. <https://doi.org/10.1007/s12035-019-1469-6>
37. Zheng Q, Kong LH, Yu CC, He RY, Wang XS, Jiang T et al. Effects of electroacupuncture on cognitive function and neuronal autophagy in rats with D-galactose induced Alzheimer's disease. *Zhen ci yan jiu*. 2020, 45(9):689-695. <https://doi.org/10.13702/j.1000-0607.190854>

**Tab. 1** Screening results of GPC's active compounds

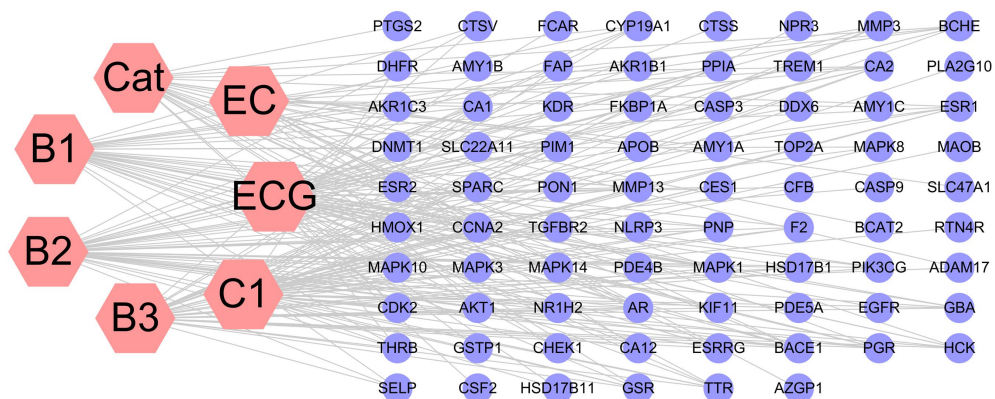
Abbreviation	Compound name	Pubchem ID
Cat	(+)-Catechin	9064
EC	(-)-Epicatechin	72276
ECG	Epigallocatechin Gallate	107905
B1	Procyanidin B1	11250133
B2	Procyanidin B2	122738
B3	Procyanidin B3	146798
C1	Procyanidin C1	169853

figure legends:

**Fig. 1** Flowchart of designed analysis in GPC treating EAE mice.



**Fig. 2** The 'Compound-target' network. Each node represents a drug target or a compound. The red nodes represent compounds and the purple nodes represent drug targets. The edge represents relationship between drug compound and target.



**Fig. 3** Network analysis of targets. (A) Venn diagram of GPC target proteins and MS target genes; (B) PPI networks for intersection targets; (C) The 'Compound-target-disease' network. Red nodes represent active compounds of GPC, green nodes represent diseases, and purple nodes represent possible targets of GPC in the treatment of MS. Each edge represents a relationship between a target and a compound or disease.

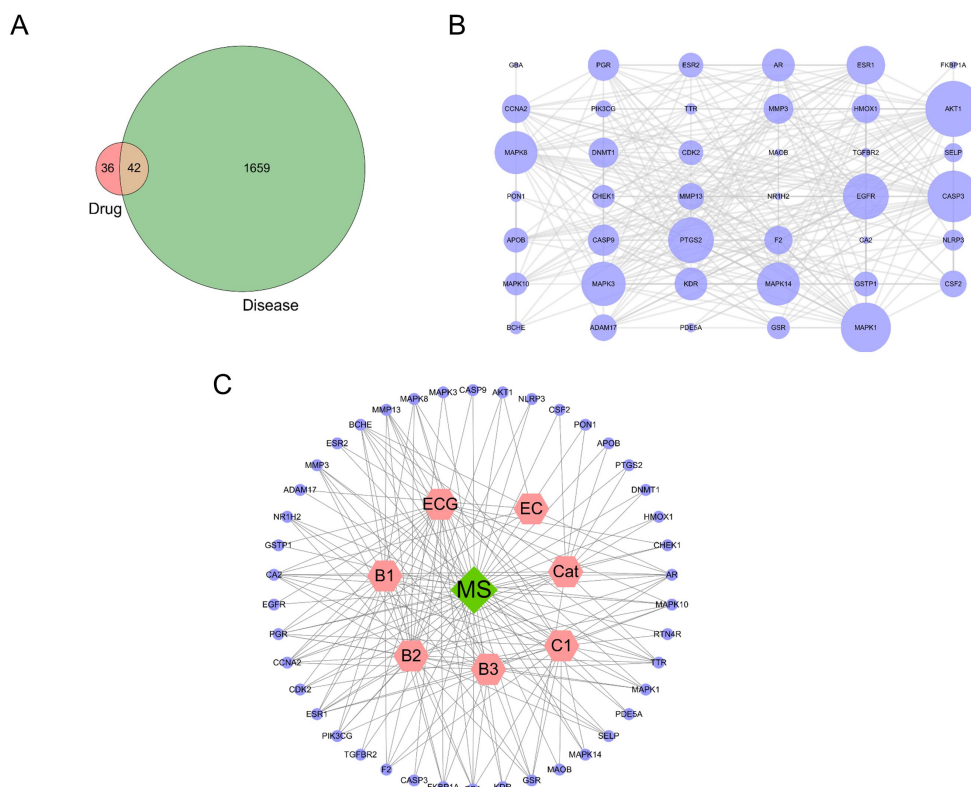


**Fig. 4** Enrichment analysis. **(A)** GO analysis; **(B)** KEGG enrichment analysis.

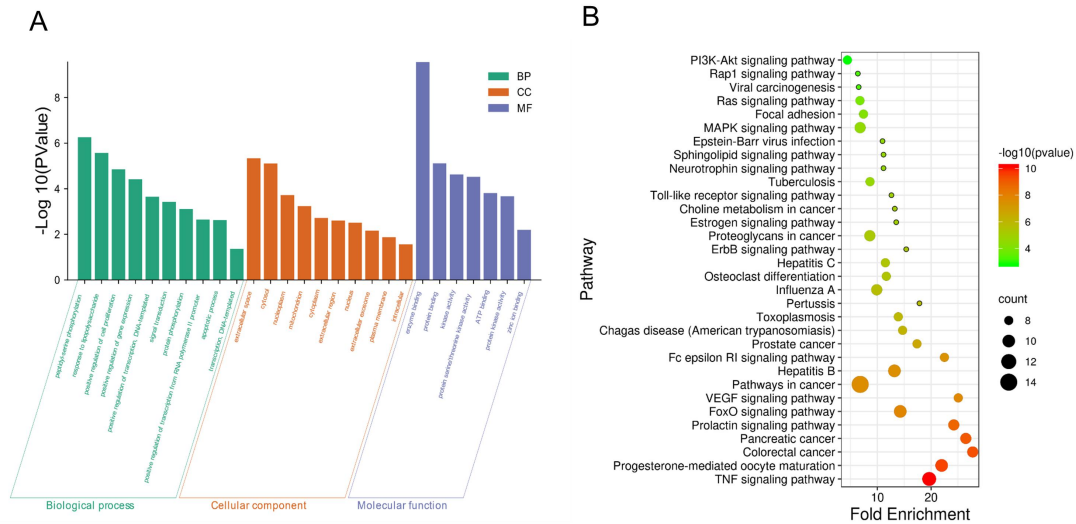


**Fig. 5** GPC ameliorates the severity of EAE, delays onset, and attenuates demyelination and inflammatory infiltration. Chronic EAE was induced in C57BL/6 mice with MOG 35-55. **(A)** Experimental flowchart: GPC was administrated 50 mg/kg by the mean of intragastric administration every day on day 3 (GPC treatment, n=6). The administration of normal saline was set up as control (EAE control, n=12). Samples collected on 28th day. **(B)** Line diagram of daily clinical neurological function score changes in the mice of two groups. **(C)** Infiltration of inflammatory cells in the spinal cord was observed by H&E staining, LFB staining was used to observe the myelin loss of the spinal cord in mice. **(D)** Immunofluorescence staining was used to observe the MBP mean fluorescence IOD of the spinal cord in mice. **(E)** The MBP relative grey value in the spinal cord in mice was observed by western blotting. Statistical significance indicated as  $*p<0.05$ ,  $**p<0.01$ ,  $***p<0.001$ .

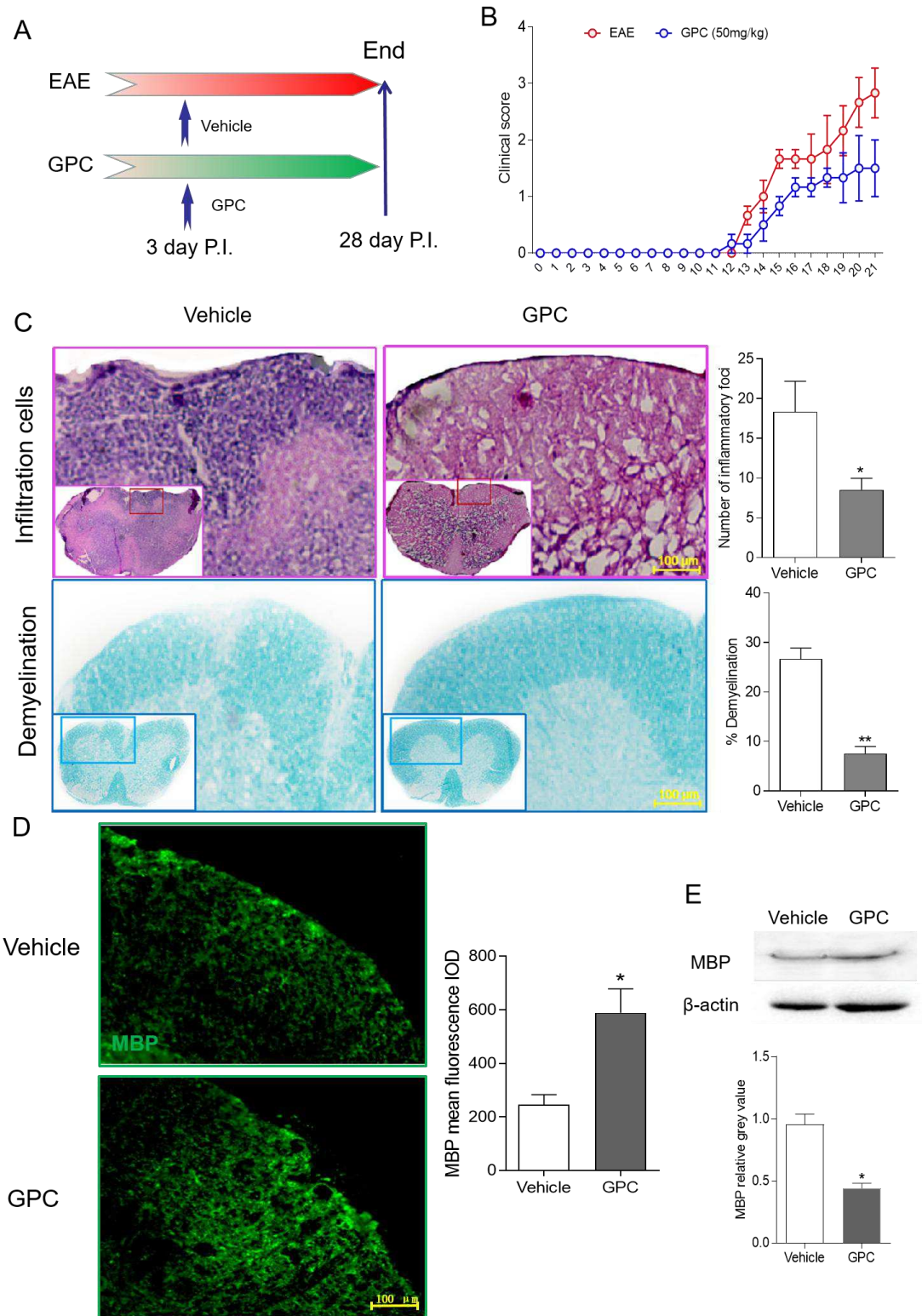


**Fig.6** Related oxidative stress indicators and pro-inflammatory cytokines in the spinal cords were measured by ELISA. **(A)** Oxidative stress indicators included SOD, MDA, RNS, ROS. **(B)** pro-inflammatory cytokines included INF- $\gamma$ , IL-17, IL-1 $\beta$ , IL-6, and TNF- $\alpha$ . Statistical analysis was

performed by one-way ANOVA followed by the Tukey Kramer test. The results are shown as the mean±SEM of triplicate determinations (\* $p$ <0.05, \*\* $p$ <0.01, \*\*\* $p$ <0.001).

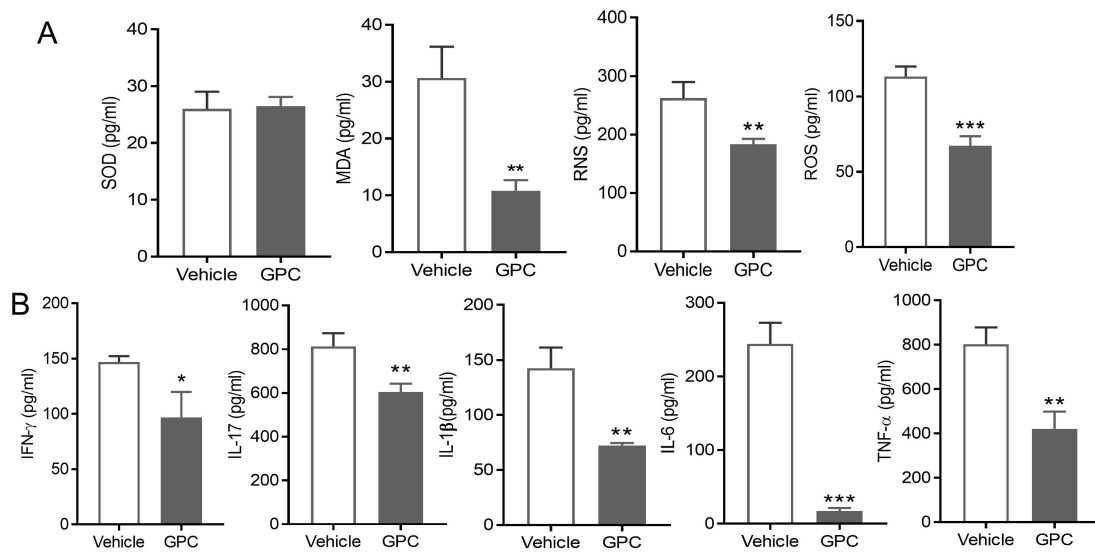
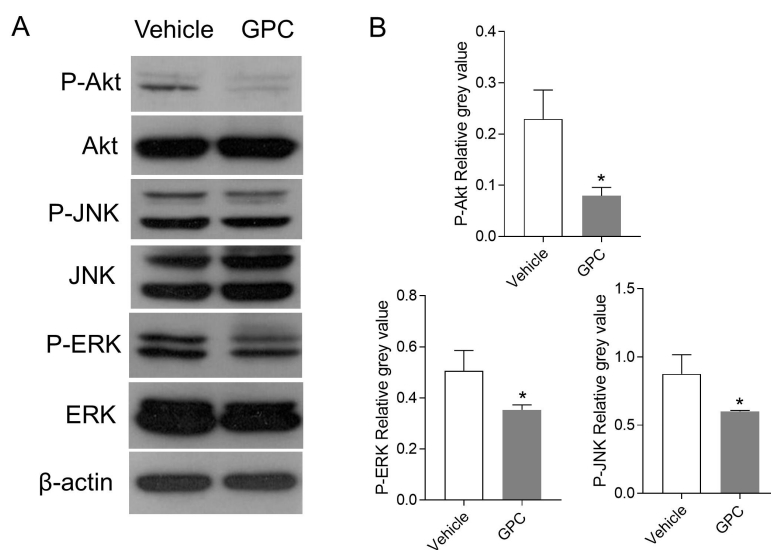


**Fig.7** GPC reduces central inflammation through the inhibition of PI3K-Akt and MAPK signaling pathway. Akt, JNK, ERK and their phosphorylation levels were analyzed by western blot analysis of the proteins, and the expressions of P-Akt, P-JNK and P-ERK were quantitatively determined by optical density using Image software, and standardized to  $\beta$ -actin levels. Statistical significance was indicated as \* $p$ <0.05, \*\* $p$ <0.01, \*\*\* $p$ <0.001.





# Figures

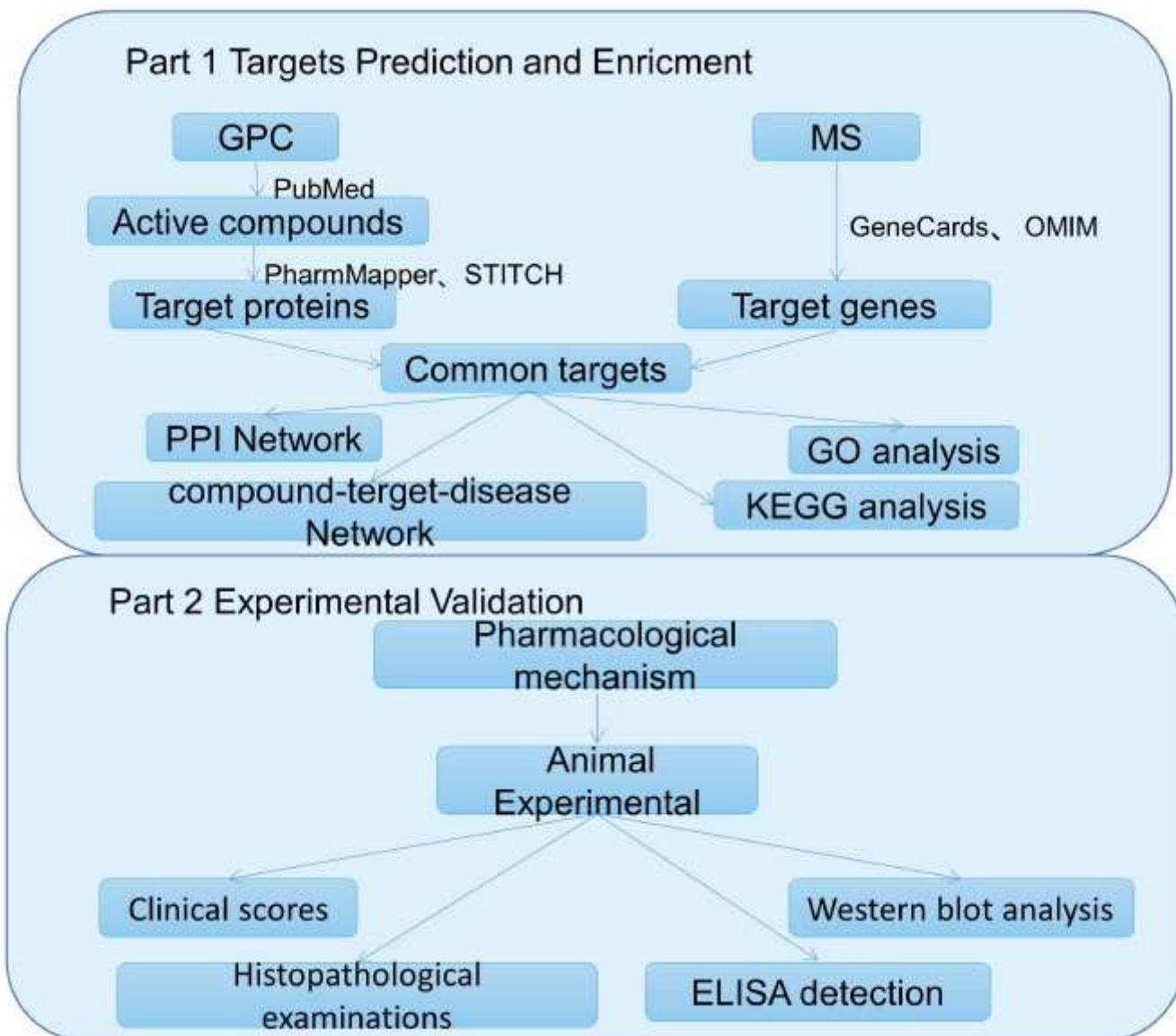
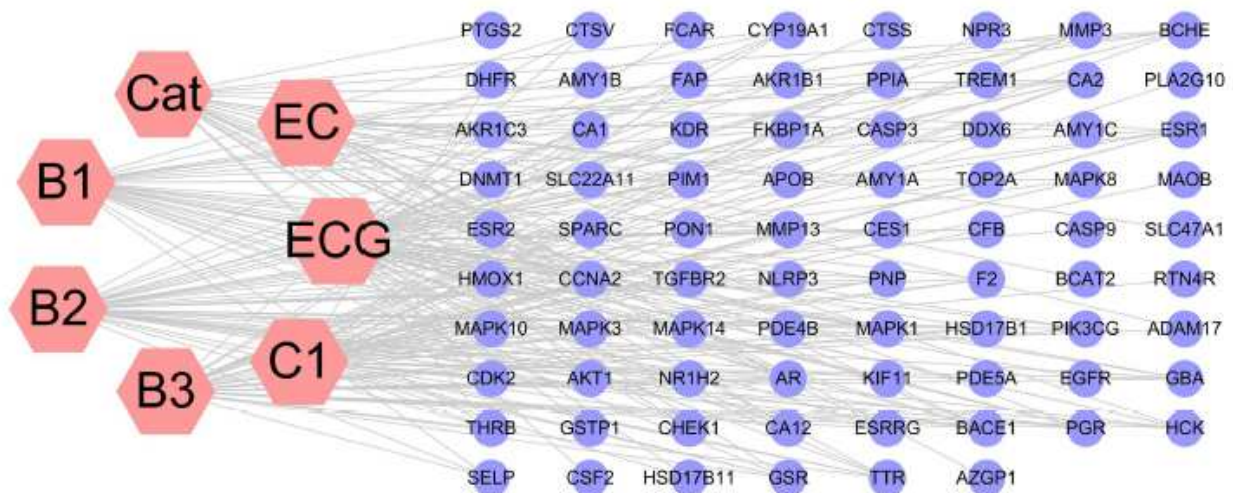


Figure 1

Flowchart of designed analysis in GPC treating EAE mice.



**Figure 2**

The 'Compound-target' network. Each node represents a drug target or a compound. The red nodes represent compounds and the purple nodes represent drug targets. The edge represents relationship between drug compound and target.

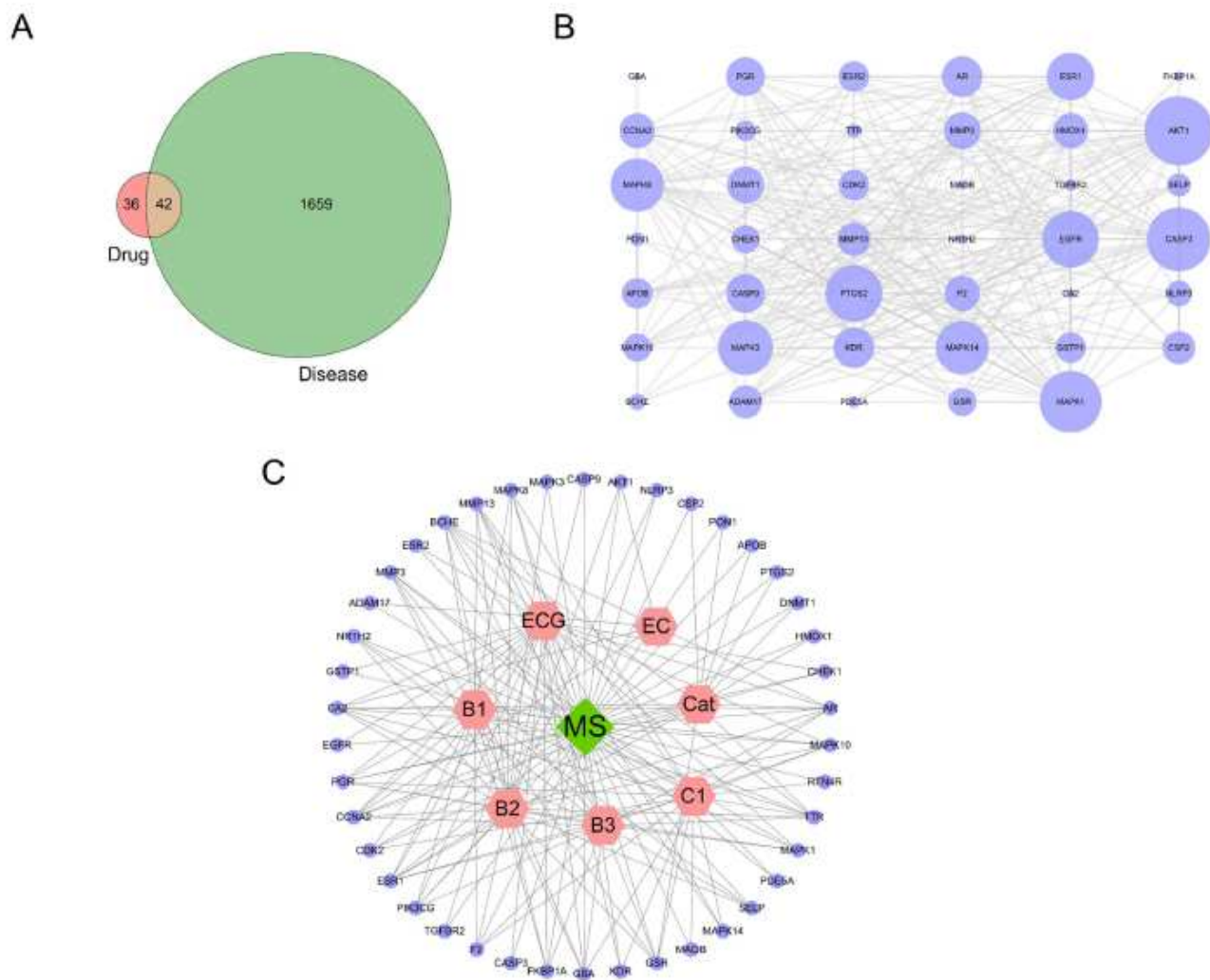


**Figure 3**

Network analysis of targets. (A) Venn diagram of GPC target proteins and MS target genes; (B) PPI networks for intersection targets; (C) The 'Compound-target-disease' network. Red nodes represent active compounds of GPC, green nodes represent diseases, and purple nodes represent possible targets of GPC in the treatment of MS. Each edge represents a relationship between a target and a compound or disease.

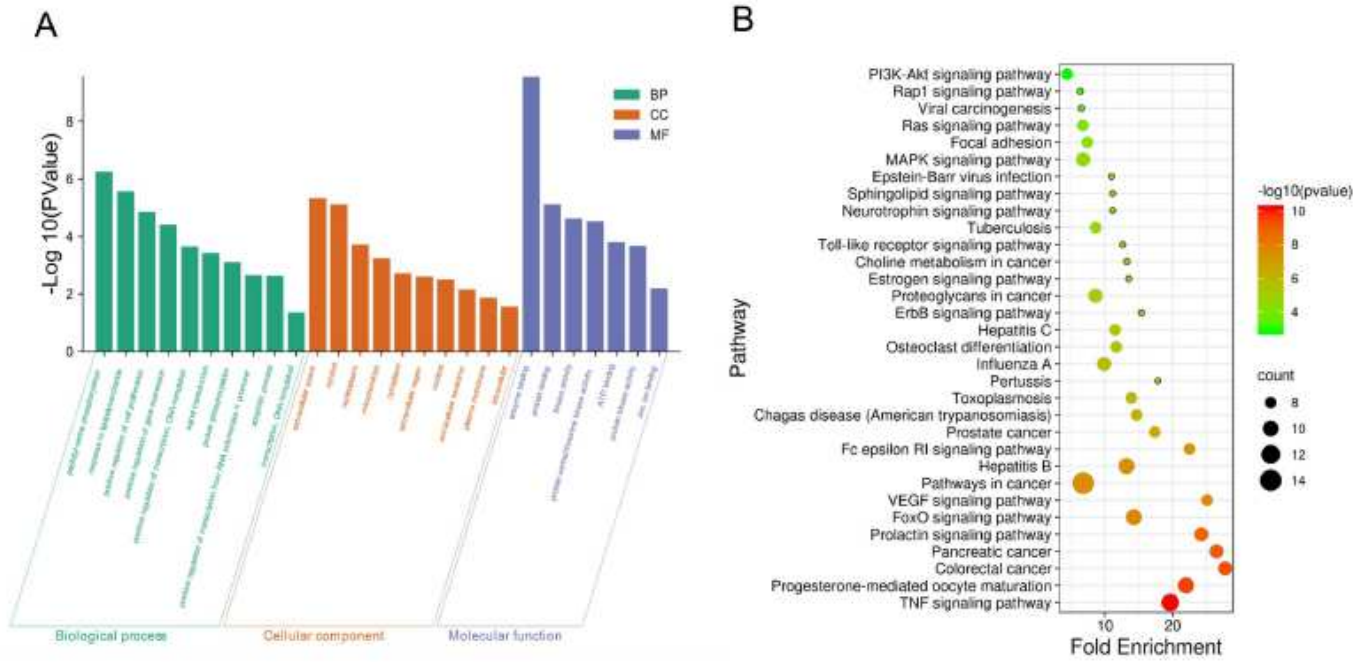


**Figure 4**

Enrichment analysis. (A) GO analysis; (B) KEGG enrichment analysis.

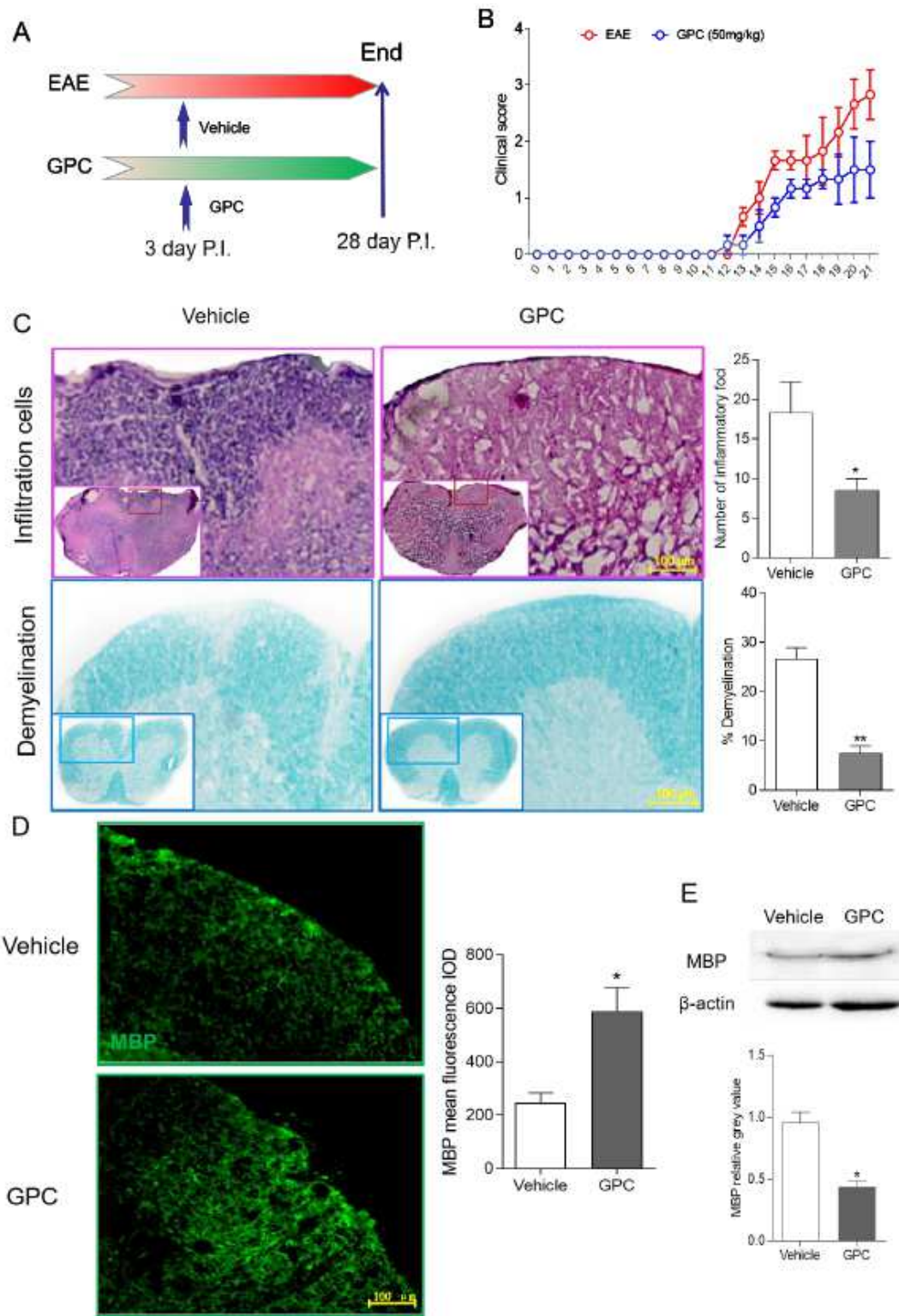


**Figure 5**

GPC ameliorates the severity of EAE, delays onset, and attenuates demyelination and inflammatory infiltration. Chronic EAE was induced in C57BL/6 mice with MOG 35-55. (A) Experimental flowchart: GPC was administered 50 mg/kg by the mean of intragastric administration every day on day 3 (GPC treatment, n=6). The administration of normal saline was set up as control (EAE control, n=12). Samples collected on 28th day. (B) Line diagram of daily clinical neurological function score changes in the mice

of two groups. (C) Infiltration of inflammatory cells in the spinal cord was observed by H&E staining, LFB staining was used to observe the myelin loss of the spinal cord in mice. (D) Immunofluorescence staining was used to observe the MBP mean fluorescence IOD of the spinal cord in mice. (E) The MBP relative grey value in the spinal cord in mice was observed by western blotting. Statistical significance indicated as \* $p < 0.05$ , \*\* $p < 0.01$ , \*\*\* $p < 0.001$ .

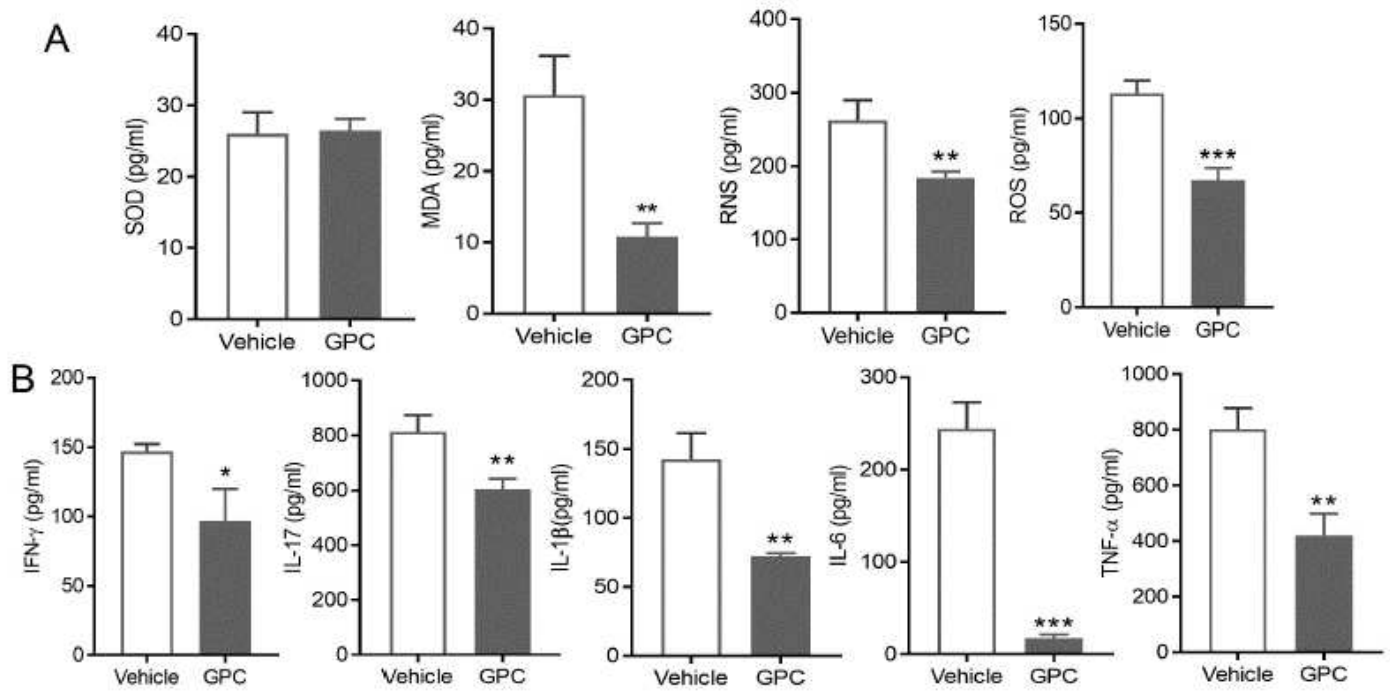


**Figure 6**

Related oxidative stress indicators and pro-inflammatory cytokines in the spinal cords were measured by ELISA. (A) Oxidative stress indicators included SOD, MDA, RNS, ROS. (B) pro-inflammatory cytokines included IFN- $\gamma$ , IL-17, IL-1 $\beta$ , IL-6, and TNF- $\alpha$ . Statistical analysis was performed by one-way ANOVA followed by the Tukey Kramer test. The results are shown as the mean $\pm$ SEM of triplicate determinations (\* $p < 0.05$ , \*\* $p < 0.01$ , \*\*\* $p < 0.001$ ).

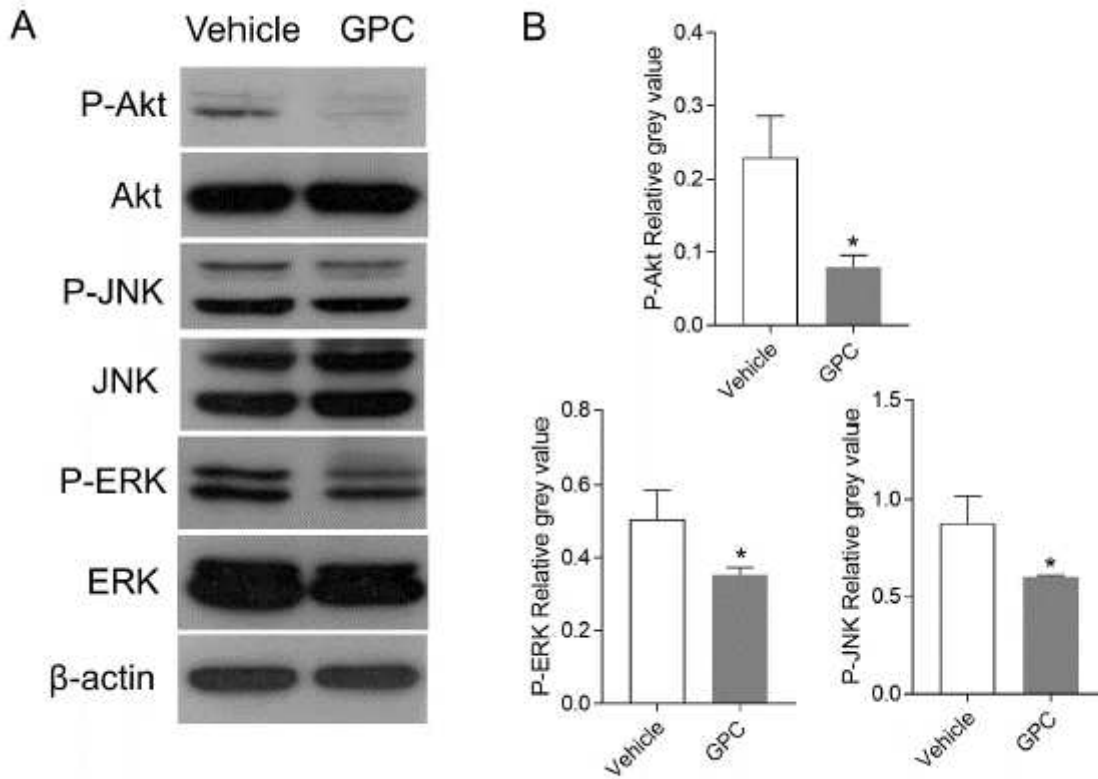


**Figure 7**

GPC reduces central inflammation through the inhibition of PI3K-Akt and MAPK signaling pathway. Akt, JNK, ERK and their phosphorylation levels were analyzed by western blot analysis of the proteins, and the expressions of P-Akt, P-JNK and P-ERK were quantitatively determined by optical density using Image software, and standardized to  $\beta$ -actin levels. Statistical significance was indicated as \* $p < 0.05$ , \*\* $p < 0.01$ , \*\*\* $p < 0.001$ .